PHILOSOPHICAL TRANSACTIONS OF THE ROYAL SOCIETY A

rsta.royalsocietypublishing.org

Research

Cite this article: Porta A, Castiglioni P, Di Rienzo M, Bassani T, Bari V, Faes L, Nollo G, Cividjan A, Quintin L. 2013 Cardiovascular control and time domain Granger causality: insights from selective autonomic blockade. Phil Trans R Soc A 371: 20120161. http://dx.doi.org/10.1098/rsta.2012.0161

One contribution of 13 to a Theme Issue 'Assessing causality in brain dynamics and cardiovascular control'.

Subject Areas:
complexity, biomedical engineering, mathematical modelling

Keywords:
Granger causality, heart rate variability, arterial pressure variability, baroreflex, autonomic nervous system, cardiovascular control

Author for correspondence:
Alberto Porta
e-mail: alberto.porta@unimi.it

Royal Society Publishing
Informing the science of the future

Cardiovascular control and time domain Granger causality: insights from selective autonomic blockade

Alberto Porta[1], Paolo Castiglioni[2], Marco Di Rienzo[2], Tito Bassani[1], Vlasta Bari[3,4], Luca Faes[5], Giandomenico Nollo[5], Andrei Cividjan[6] and Luc Quintin[6]

[1]Department of Biomedical Sciences for Health, Galeazzi Orthopaedic Institute, University of Milan, 20161 Milan, Italy
[2]Don Carlo Gnocchi Foundation, 20162 Milan, Italy
[3]Department of Bioengineering, Politecnico di Milano, 20133 Milan, Italy
[4]Gruppo Ospedaliero San Donato Foundation, 20122 Milan, Italy
[5]Department of Physics and BIOtech, University of Trento, 38060 Mattarello, Trento, Italy
[6]Physiology (EA 4612: Neurocardiology), University of Lyon, 69365 Lyon, France

We studied causal relations among heart period (HP), systolic arterial pressure (SAP) and respiration (R) according to the definition of Granger causality in the time domain. Autonomic pharmacological challenges were used to alter the complexity of cardiovascular control. Atropine (AT), propranolol and clonidine (CL) were administered to block muscarinic receptors, β-adrenergic receptors and centrally sympathetic outflow, respectively. We found that: (i) at baseline, HP and SAP interacted in a closed loop with a dominant causal direction from HP to SAP; (ii) pharmacological blockades did not alter the bidirectional closed-loop interactions between HP and SAP, but AT reduced the dominance of the causal direction from HP to SAP; (iii) at baseline, bidirectional interactions between HP and R were frequently found; (iv) the closed-loop relation between HP and R was unmodified by the administration of drugs; (v) at baseline, unidirectional interactions from R to SAP were often found; and (vi) while AT induced frequently an uncoupling between R and SAP, CL favoured bidirectional interactions.

These results prove that time domain measures of Granger causality can contribute to the description of cardiovascular control by suggesting the temporal direction of the interactions and by separating different causality schemes (e.g. closed loop versus unidirectional relations).

1. Introduction

The traditional experimental approach to the inference of causality is based on the application of an external stimulus to the system under study and the observation of its causally related response. For example, in the field of the analysis of cardiovascular control, sinusoidal breathing at different discrete frequencies was originally used to drive respiratory-related heart rate changes [1]. This approach was recently extended using a random breathing pattern, thus estimating the relation from respiration to heart rate changes over a continuous range of breathing rates [2]. Examples of applications of the perturbational method to assess causal relations include electrical stimulation of vagal and sympathetic efferent activity directed to the heart to drive heart rate modifications [3,4], electrical stimulation of sympathetic nerves directed to vascular smooth muscles to evoke skin blood flow changes [5] and perturbations of the carotid sinuses with random binary pressure pulses to evoke sympathetic responses and peripheral vasoconstriction [6]. This traditional approach led to important theoretical advances [7] and had relevant practical applications [8] but left completely unsolved the issue of assessing causal relations during spontaneous activity. Indeed, knowledge of the causal interactions when the system is under an external perturbation does not necessarily imply mastering the system functioning under spontaneous conditions. Moreover, the external stimulation is frequently not natural, and thus the system functioning is explored in artificial conditions. Even when using a physiological probe, such as respiration, the collaboration of the subject necessary to reproduce a specific pattern may change the operational set point of the system with respect to spontaneous conditions. As a further drawback, the perturbational approach is unsuitable for studying complex causality schemes. Indeed, the magnitude of the stimulation necessary to evoke a clearly driven response might be so important as to make impracticable the recognition of any activity due to the presence of feedback. For example, the large pressure change induced by the administration of a vasoactive drug necessary to evoke an evident heart rate variation during the assessment of baroreflex sensitivity [9] prevents any possibility to disentangle the reflex modification of arterial pressure provoked by the drug-induced heart rate variation [10]. Finally, there are systems that cannot be stimulated for ethical reasons without any evident therapeutic indication (e.g. subthalamic nucleus in Parkinson disease) or due to the impossibility for humans to intervene (e.g. climate).

The definition of causality provided by Granger [11] opened the field of the analysis of causality in spontaneous conditions. The operative definition of causality given by Granger is that a time series y_k Granger-causes another time series y_m if the prediction of y_m obtained from the most complete set of information we have about the system functioning is significantly better than that derived from the same set of information after excluding y_k. Applications of this approach to the study of cardiovascular control based on spontaneous beat-to-beat fluctuations of cardiovascular variables allowed the identification of physiological mechanisms known to operate along well-defined temporal directions [12–15] and the assessment of the strength of the inferred causal relationships [16,17]. It was proposed that cardiovascular control makes use of strategies of selection of causality patterns to increase its flexibility in the presence of changeable conditions and its swiftness in reacting to risky situations [18]. Among these strategies, we suggested the possibility of modulating the dominance of a causal relation in closed-loop interactions [12,18] and of inducing a progressive decoupling of cardiovascular variables from respiratory influences [18].

The aim of this study is to investigate the role played by the autonomic nervous system in modulating causality in cardiovascular control by exploiting a pharmacological protocol devised

to selectively block sympathetic and parasympathetic branches of the autonomic nervous system [19]. Granger causality was assessed in the time domain [11] according to the comparison of the predictability of the presumed 'effect' series based on the most complete information set describing the system functioning with that derived after excluding the presumed 'cause' series from the information set.

2. Material and methods

(a) Evaluating Granger causality and directionality in the time domain

Given the series $Y_1 = \{Y_1(n),\ n = 1, \ldots, N\}$, $Y_2 = \{Y_2(n),\ n = 1, \ldots, N\}, \ldots, Y_M = \{Y_M(n),\ n = 1, \ldots, N\}$, where n is the progressive counter and N is the series length, they are first normalized, thus obtaining $y_1, y_2, \ldots, y_M$ series with zero mean and unit variance. The set of M signals, $\Omega = \{y_1, \ldots, y_{m-1}, y_m, y_{m+1}, \ldots, y_M\}$, represents the universe of our knowledge about the system under examination. According to the class of the multivariate autoregressive models [20], the interactions among the M signals in Ω can be described as

$$y(n) = A(z) \cdot y(n) + w(n), \tag{2.1}$$

where $y = [y_1 \ldots y_M]^{\mathrm{T}}$ is the column vector of the signals (the superscript 'T' indicates the transpose operator), $w = [w_1 \ldots w_M]^{\mathrm{T}}$ is the column vector of uncorrelated white noises each with zero mean and variance λ_m^2, with $m = 1, \ldots, M$, $A(z)$ is the $M \times M$ matrix of the causal finite impulse response filters describing the interactions among signals and z is the forward shift operator (i.e. $z \cdot y_k(n) = y_k(n+1)$) [20]. The matrix $A(z)$ can be written as

$$A(z) = \sum_{i=0}^{p} A_i \cdot z^{-i}, \tag{2.2}$$

where A_i is the $M \times M$ matrix containing, on the main diagonal, the coefficients $a_{kk}(i)$ with $1 \le k \le M$ describing the auto-dependence of $y_k(n)$ on $y_k(n-i)$ in Ω and, outside the main diagonal, the coefficients $a_{kl}(i)$ with $l \ne k$ and $1 \le k, l \le M$ describing the cross-dependence of $y_k(n)$ on $y_l(n-i)$ in Ω. Equation (2.2) is helpful to put in evidence A_0. According to the structure given to A_0, immediate effects between any pair of signals can be imposed. While immediate effects of y_k on itself are not allowed (i.e. $a_{kk}(0) = 0$) to avoid the impractical situation of self-loops without delay, the instantaneous effects of y_k on y_l might be allowed by identifying $a_{kl}(0)$. If $a_{kl}(0) \ne 0$ is found, special attention must be paid to impose $a_{lk}(0) = 0$ to avoid the formation of loops involving different variables without delays [16,21]. Usually, A_0 is imposed equal to 0 everywhere, thus supposing that immediate effects are irrelevant in setting causality as a consequence of the long latency of the possible influences between any pair of signals in Ω compared with the sampling period. However, this is not the case in the analysis of the cardiovascular control based on spontaneous variabilities due to the convention used to measure variables on a beat-to-beat basis [16,21,22]. The coefficients of $A(z)$ can be identified according to some optimization criterion applied to y (e.g. the minimization of the determinant of the covariance matrix of w [20]), thus leading to the computational estimate of $A(z)$, $\hat{A}(z)$. The prediction of $y(n)$, $\hat{y}(n)$, can be obtained by filtering $y(n)$ with $\hat{A}(z)$ as

$$\hat{y}(n) = \hat{A}(z) \cdot y(n). \tag{2.3}$$

Defining $\Omega - \{y_m\} = \{y_1, \ldots, y_{m-1}, y_{m+1}, \ldots, y_M\}$ as the universe Ω after excluding y_m, equation (2.1) holds again provided that y_m is excluded from y (i.e. $y = [y_1 \ldots y_{m-1}\ \ y_{m+1} \ldots y_M]^{\mathrm{T}}$), w_m is excluded from w (i.e. $w = [w_1 \ldots w_{m-1} w_{m+1} \ldots w_M]^{\mathrm{T}}$) and the mth row and column are excluded from $A(z)$ (i.e. $A_{mj}(z)$ and $A_{jm}(z)$ with $1 \le j \le M$ are excluded from $A(z)$). The application of the identification procedure in $\Omega - \{y_m\}$ leads to the evaluation of $\hat{y} = [\hat{y}_1 \ldots \hat{y}_{m-1} \hat{y}_{m+1} \ldots \hat{y}_M]^{\mathrm{T}}$ that does not include the prediction of y_m. Defining the prediction error, $e_k(n)$, as the difference between $y_k(n)$ and its prediction, $\hat{y}_k(n)$, the mean squared prediction error over N samples can be assessed in Ω and in $\Omega - \{y_m\}$ and indicated as $\hat{\lambda}_k^2|_{\Omega}$ and $\hat{\lambda}_k^2|_{\Omega - \{y_m\}}$, respectively. According

to the Granger causality approach, y_m Granger-causes y_k in Ω, in the following indicated as $y_m \rightarrow y_k$, if $\hat{\lambda}^2_k|_{\Omega-\{y_m\}}$ is significantly larger than $\hat{\lambda}^2_k|_{\Omega}$ (i.e. the exclusion of y_m from Ω worsens the prediction of y_k) [11]. The traditional F-test is commonly used to contrast $\hat{\lambda}^2_k|_{\Omega-\{y_m\}}$ and $\hat{\lambda}^2_k|_{\Omega}$ [23]. Reversing the role of y_m and y_k allows the assessment of $y_k \rightarrow y_m$. If both $y_m \rightarrow y_k$ and $y_k \rightarrow y_m$ are contemporaneously found, a closed-loop relation (bidirectional causality) can be argued (i.e. $y_m \leftrightarrow y_k$). If the null hypothesis that y_m does not Granger-cause y_k and vice versa cannot be rejected, y_m and y_k are uncoupled. F-test was performed with $p < 0.01$.

The assessment of the dominant causality can be based on a direct comparison between F values assessed over opposite causal directions. Accordingly, the directionality index (DI) [24] is defined as

$$\mathrm{DI}_{km} = F_{km} - F_{mk}, \tag{2.4}$$

where F_{km} and F_{mk} represent the F values assessed from y_m to y_k and vice versa, respectively [23]. $\mathrm{DI}_{km} > 0$ indicates that the causal direction from y_m to y_k is prevalent over the reverse one, while $\mathrm{DI}_{km} < 0$ points out the opposite situation. DI_{km} is exclusively capable of identifying the dominant causality: indeed, $\mathrm{DI}_{km} > 0$ or $\mathrm{DI}_{km} < 0$ does not exclude bidirectional interactions. In addition, DI_{km} close to 0 might indicate: (i) a full uncoupling between y_k and y_m; (ii) closed-loop interactions between y_k and y_m with none of the causal directions taking real pre-eminence; and (iii) synchronization between y_k and y_m.

3. Experimental protocol and data analysis

(a) Experimental protocol

We exploited data recorded during an experimental protocol planned to study the effects of pharmacological blockades of the parasympathetic and sympathetic branches of the autonomic nervous system on the baroreflex sensitivity [19]. We make reference to Parlow *et al*. [19] for a detailed description of the experimental protocol. Briefly, we studied nine healthy male physicians aged from 25 to 46 years familiar with the study setting. None had any abnormal finding in history, physical examination or electrocardiography or was receiving any medication. All had normal resting brachial arterial pressure measured by sphygmomanometer. They were instructed to avoid tobacco, alcohol and caffeine for 12 h and strenuous exercise for 24 h before each experiment. All the subjects gave their written informed consent. Experimental sessions were performed in 3 days at approximately two-week intervals. Subjects remained at rest in supine position in a quiet darkened room during all the recordings. Each experiment consisted of 15–20 min of baseline recording followed by 15–20 min of recording after drug administration. Recordings were obtained as follows: (i) on day 1, after parasympathetic blockade with $40\,\mu g\,kg^{-1}$ intravenous (IV) atropine (AT) sulfate to block muscarinic receptors; (ii) on day 2, after β-adrenergic blockade with $200\,\mu g\,kg^{-1}$ IV propranolol (PR) to block β_1 cardiac and β_2 vascular peripheral adrenergic receptors; (iii) on day 1, PR was administered at the end of the AT session (the dose of AT was reinforced by $10\,\mu g\,kg^{-1}$) to combine the effect of AT and PR (AT + PR) and obtain a cardiac parasympathetic and sympathetic blockade; and (iv) on day 3, 120 min after $6\,\mu g\,kg^{-1}$ per os clonidine (CL) hydrochloride to centrally block the sympathetic outflow to the heart and vasculature and to centrally increase the cardiac parasympathetic activity [25]. Since one volunteer took part only in the first day experiments, the total number of recordings were 25, 9, 9, 8 and 8 at baseline and after AT, AT + PR, PR and CL, respectively. The protocol adhered to the principles of the Declaration of Helsinki. The human research and ethical review board of the Hospices Civils de Lyon approved the protocol.

(b) Data collection and variability series extraction

Electrocardiogram (ECG) and non-invasive finger blood pressure (Finapres 2300, Ohmeda) were recorded during the experiments. The hand of the subject was kept at the level of the heart.

Signals were sampled at 500 Hz. After detecting the QRS complex (the ventricular depolarization waveform) on the ECG and locating its apex using parabolic interpolation, the temporal distance between two consecutive QRS parabolic apexes was computed and used as an approximation of heart period (HP). The maximum of arterial pressure inside HP was taken as systolic arterial pressure (SAP). Since respiration (R) modulates the amplitude of the ECG waveform, the area of the QRS complex assessed with respect to the isoelectric baseline (B) was exploited to infer R [26]. The occurrences of QRS and SAP peaks were carefully checked to avoid erroneous detections or missed beats. If isolated ectopic beats affected HP and SAP values, these measures were linearly interpolated using the closest values unaffected by ectopic beats. $\mathrm{HP} = \{\mathrm{HP}(n), n = 1, \ldots, N\}$, $\mathrm{SAP} = \{\mathrm{SAP}(n), n = 1, \ldots, N\}$ and $\mathrm{R} = \{\mathrm{R}(n), n = 1, \ldots, N\}$ were extracted on a beat-to-beat basis, where n was the progressive cardiac beat number, and N was the series length. SAP(n) was taken inside HP(n). R(n) was computed over the first QRS delimiting HP(n). The series were linearly detrended. Sequences of 256 consecutive measures were randomly selected inside B, AT, PR, AT + PR and CL periods, thus focusing on short-term cardiovascular control mechanisms [27]. If evident non-stationarities, such as very slow drifting of the mean or sudden changes of the variance, were present despite the linear detrending, the random selection was carried out again. The mean and the variance of HP and SAP were indicated as μ_{HP}, μ_{SAP}, σ^2_{HP} and σ^2_{SAP}, and expressed in ms, mmHg, ms^2 and mmHg^2, respectively. The per cent power in the respiratory band (from 0.15 to 0.5 Hz) and the dominant respiratory frequency were monitored as well (i.e. RP% and RF) and expressed as per cent units and Hz, respectively.

(c) Identification of the model parameters from cardiovascular variabilities

Given $y_1 = \mathrm{hp}$, $y_2 = \mathrm{sap}$ and $y_3 = \mathrm{r}$, the coefficients of the polynomials, $A_{kl}(z)$ with $1 \le k, l \le 3$, were identified both in $\Omega = \{y_1, y_2, y_3\}$ and in $\Omega - \{y_k\}$ with $k = 1, 2, 3$ directly from cardiovascular series using the traditional least-squares approach and Cholesky decomposition method [20,21]. The delays τ_{12} and τ_{13} were set to 0 to allow the description of the fast vagal reflex (within the same cardiac beat) capable of modifying HP in response to changes of SAP and R [23,28]. The delay τ_{23} was set to 0 to account for the rapid effect of R on SAP due to the immediate transfer of an alteration of intrathoracic pressure on SAP value [29]. The delay τ_{21} was set to 1 to describe the one-beat delayed effect of HP on SAP due to the measurement conventions preventing HP(n) modifying of SAP(n) [30]. According to Saul *et al*. [2,7], the actions of HP and SAP on R are slower (i.e. they cannot occur in the same beat), thus leading to $\tau_{31} = 1$ and $\tau_{32} = 1$. As a result of this choice, A_0 was upper triangular with all zeros on the main diagonal and below it. The same setting for instantaneous causality relations was imposed by Faes *et al*. [22]. The model order, p, was optimized in the range from 4 to 16 according to the Akaike figure of merit for multivariate processes [31]. The coefficients of $A(z)$ were obtained by minimizing the determinant of the covariance matrix of $w = [w_1 \quad w_2 \quad w_3]^{\mathrm{T}}$. Whiteness of the residuals, w_k with $1 \le k \le 3$, and their uncorrelation, even at zero lag, were tested. The optimal model order chosen in Ω was maintained even in $\Omega - \{y_k\}$ with $k = 1, 2, 3$, but the coefficients of the polynomials were estimated again.

(d) Statistical analysis

Kruskal–Wallis one-way analysis of variance on ranks was applied (Dunn's test) to check whether parameters changed after drug administration. A $p < 0.05$ was considered significant.

4. Results

Figure 1 shows an example of HP, SAP and R series recorded at B (figure 1*a–c*), after AT (figure 1*d–f*), after PR (figure 1*g–i*), after AT + PR (figure 1*j–l*) and after CL (figure 1*m–o*) in the same subject. HP is remarkably lower after AT (figure 1*d*) and AT + PR (figure 1*j*) and higher after PR (figure 1*g*) and CL (figure 1*m*). The magnitude of the HP variability dramatically decreases after AT (figure 1*d*) and AT + PR (figure 1*j*), especially the amplitude of fast oscillations. SAP

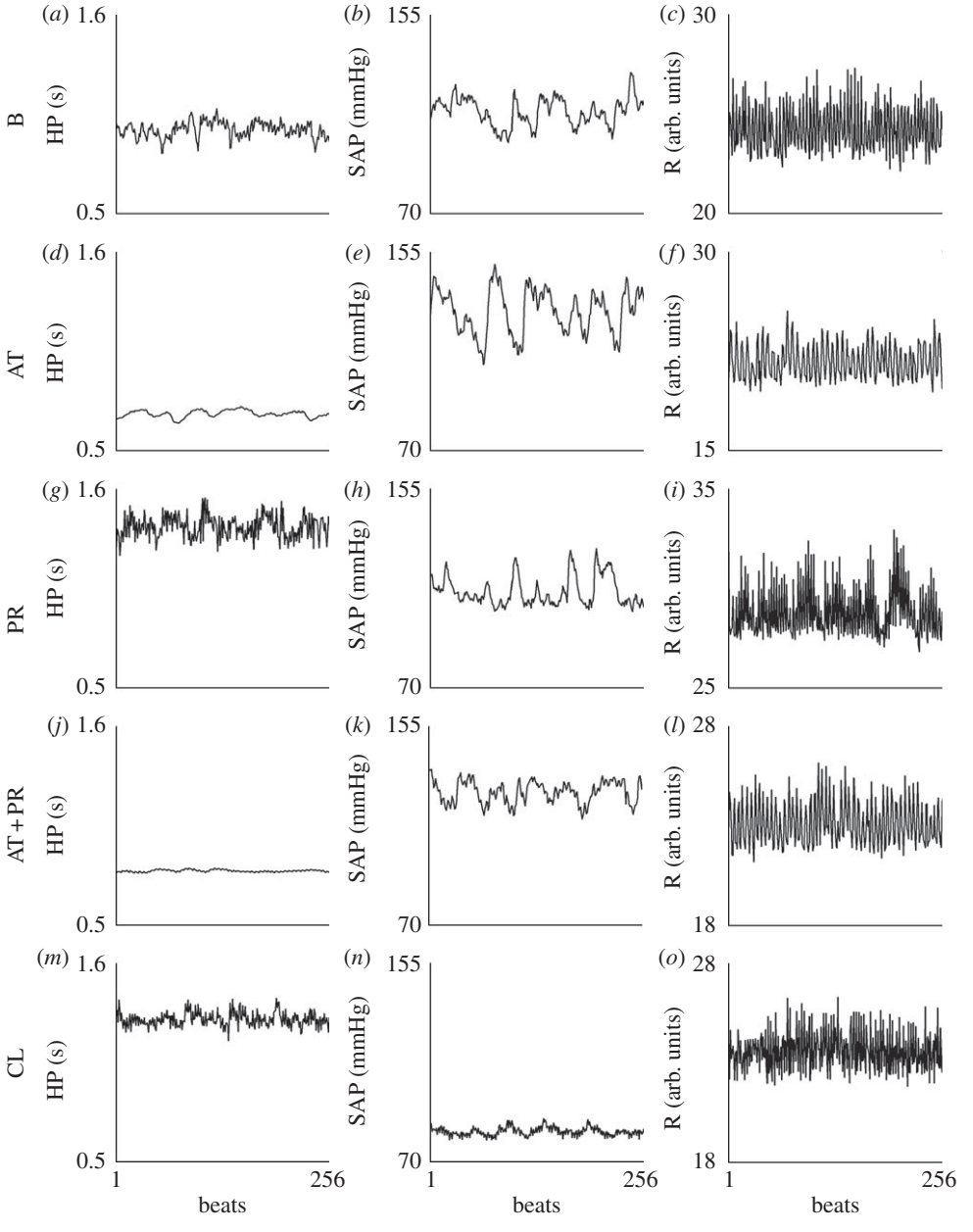

Figure 1. Series of HP (*a*,*d*,*g*,*j*,*m*), SAP (*b*,*e*,*h*,*k*,*n*) and R (*c*,*f*,*i*,*l*,*o*) recorded from the same subject at B (*a*,*b*,*c*), after AT (*d*,*e*,*f*), after PR (*g*,*h*,*i*), after AT + PR (*j*,*k*,*l*) and after CL (*m*,*n*,*o*). RF is 0.26, 0.24, 0.25, 0.25, 0.27 Hz at B and after AT, PR, AT + PR and CL, respectively. Please note that, because the heart rate differs among conditions, horizontal axes of 256 beats actually correspond to different time spans.

is significantly increased after AT (figure 1*e*) and AT + PR (figure 1*k*), whereas the magnitude of SAP variability dramatically decreases after CL (figure 1*n*), especially the amplitude of slow oscillations. Respiratory-related oscillations are clearly visible in the R series in all the experimental conditions (figure 1*c*,*f*,*i*,*l*,*o*) with an RF ranging from 0.24 Hz after AT to 0.27 Hz after CL. These observations were confirmed over the entire group of subjects (figure 2). The HP mean, μ_{HP}, was significantly affected by all the experimental conditions, although in a different way: indeed, after AT and AT + PR, μ_{HP} significantly decreased (figure 2*a*), while μ_{HP}

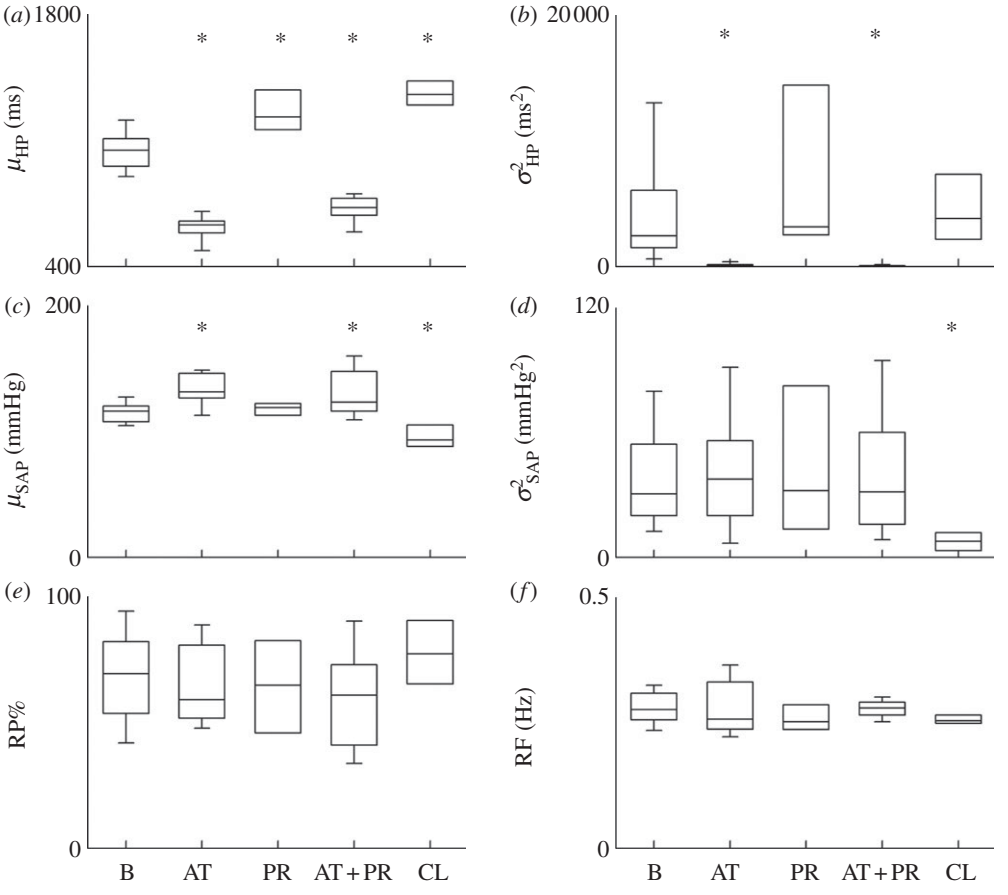

Figure 2. Box-and-whiskers plots report the 10th, 25th, 50th, 75th and 90th percentiles of the (*a*) HP mean, μ_{HP}, (*b*) HP variance, σ^2_{HP}, (*c*) SAP mean, μ_{SAP}, (*d*) SAP variance, σ^2_{SAP}, (*e*) per cent power of the respiratory signal in the respiratory band, RP%, and (*f*) dominant respiratory frequency, RF, at B and after AT, PR, AT + PR and CL. Asterisk indicates a significant change compared with B.

increased after PR and CL (figure 2*a*). The HP variance, σ^2_{HP}, was virtually abolished after AT and AT + PR (figure 2*b*). The SAP mean, μ_{SAP}, was significantly increased after AT and AT + PR, and decreased after CL (figure 2*c*). Only CL produced a significant variation of the SAP variance, σ^2_{SAP} (figure 2*d*). The per cent power of the respiratory signal in the respiratory band, RP%, and the dominant respiratory frequency, RF, were insignificantly affected by the pharmacological challenges (figure 2*e*,*f*).

Results of causality analysis between y_1 (i.e. hp) and y_2 (i.e. sap) are shown in figure 3. While the F value assessing causality from y_2 to y_1, F_{12}, was not affected by the drug administration (figure 3*a*), the F value evaluating causality from y_1 to y_2, F_{21}, significantly decreased after AT and AT + PR (figure 3*b*). The large decrease of F_{21} after AT and AT + PR led to a significant decrease of DI_{21} as well (figure 3*c*). At B, DI_{21} was larger than 0 in 100 per cent of the subjects (figure 3*c*), thus indicating a dominant causality from y_1 to y_2. Even though the percentage of subjects with $DI_{21} > 0$ was smaller after the administration of the drugs (i.e. 89%, 75%, 67% and 75% after AT, PR, AT + PR and CL, respectively), causality from y_1 to y_2 remained prevalent.

Findings of causality analysis between y_1 (i.e. hp) and y_3 (i.e. r) are shown in figure 4. Both the F values assessing causality from y_3 to y_1, F_{13}, and from y_1 to y_3, F_{31}, were not modified by the administration of the drugs (figure 4*a*,*b*). DI_{31} remained constant as well in all the experimental conditions (figure 4*c*). At B, DI_{31} was larger than 0 in 56 per cent of the subjects, thus indicating

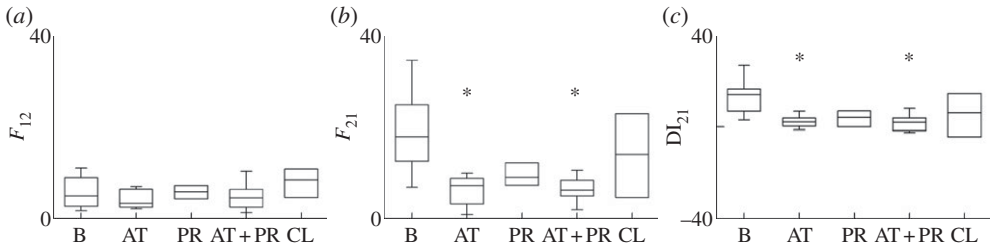

Figure 3. Box-and-whiskers plots report the 10th, 25th, 50th, 75th and 90th percentiles (*a*) of the predictability improvement of y_1 due to the introduction of y_2, F_{12}, (*b*) of the predictability improvement of y_2 due to the introduction of y_1, F_{21}, and (*c*) of the directionality index, DI_{21}, at B and after AT, PR, AT + PR and CL with $y_1 =$ hp and $y_2 =$ sap. Asterisk indicates a significant change compared with B.

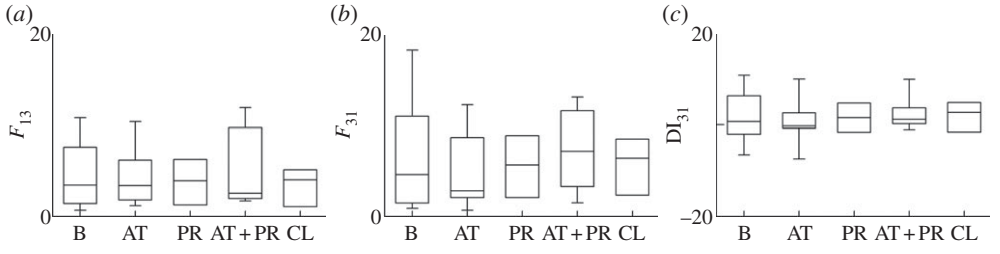

Figure 4. Box-and-whiskers plots report the 10th, 25th, 50th, 75th and 90th percentiles (*a*) of the predictability improvement of y_1 due to the introduction of y_3, F_{13}, (*b*) of the predictability improvement of y_3 due to the introduction of y_1, F_{31}, and (*c*) of the directionality index, DI_{31}, at B and after AT, PR, AT + PR and CL with $y_1 =$ hp and $y_3 =$ r. No significant change compared with B was detected.

that none of the two causal relations were prevalent. After AT, the percentage of $DI_{31} > 0$ was slightly smaller than 50 per cent (i.e. 44%), whereas it increased above 50 per cent after PR, AT + PR and CL (i.e. 75%, 78% and 63%, respectively).

Results of causality analysis between y_2 (i.e. sap) and y_3 (i.e. r) are shown in figure 5. Pharmacological challenges did not influence either the F value assessing causality from y_3 to y_2, F_{23}, or that evaluating causality from y_2 to y_3, F_{32} (figure 5*a*,*b*). DI_{32} was unmodified in all the experimental conditions as well (figure 5*c*). At B, DI_{32} was larger than 0 in a negligible percentage of subjects (i.e. 28%), thus indicating the dominance of the causal link from y_3 to y_2. The percentage of subjects with $DI_{32} > 0$ remained low in all the experimental conditions (i.e. 33%, 13%, 33% and 13% after AT, PR, AT + PR and CL, respectively).

Figure 6 shows the rates of detection of causality patterns as a function of the experimental condition. A closed-loop relation between y_1 and y_2, $y_1 \leftrightarrow y_2$, was found in a large fraction of subjects at B (i.e. 72%; figure 6*a*, solid bar). This fraction was above 50 per cent in all the pharmacological challenges (67%, 100%, 56% and 88% after AT, PR, AT + PR and CL, respectively) and was not significantly affected by the administration of drugs. The percentage of subjects with solely unidirectional causality along baroreflex (i.e. $y_2 \rightarrow y_1$) or with uncoupling between y_1 and y_2 was negligible (figure 6*a*) in all experimental conditions. At B, the percentage of subjects with closed-loop relation between y_1 and y_3, $y_1 \leftrightarrow y_3$ (figure 6*b*, solid bar), was significant (i.e. 52%). This causality pattern dominated over the other ones in all the experimental conditions and its importance was not modified by the administration of drugs (44%, 63%, 56% and 50% after AT, PR, AT + PR and CL, respectively). Results of causality analysis between y_2 and y_3 strongly depended on the experimental conditions (figure 6*c*). Unidirectional causality from y_3 to y_2 (figure 6*c*, backslash-pattern bar) was the most frequently found causality scheme at B

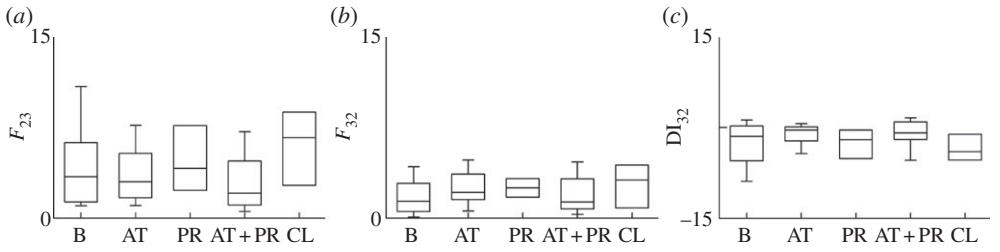

Figure 5. Box-and-whiskers plots report the 10th, 25th, 50th, 75th and 90th percentiles (*a*) of the predictability improvement of y_2 due to the introduction of y_3, F_{23}, (*b*) of the predictability improvement of y_3 due to the introduction of y_2, F_{32}, and (*c*) of the directionality index, DI_{32}, at B and after AT, PR, AT + PR and CL with $y_2 =$ sap and $y_3 =$ r. No significant change compared with B was detected.

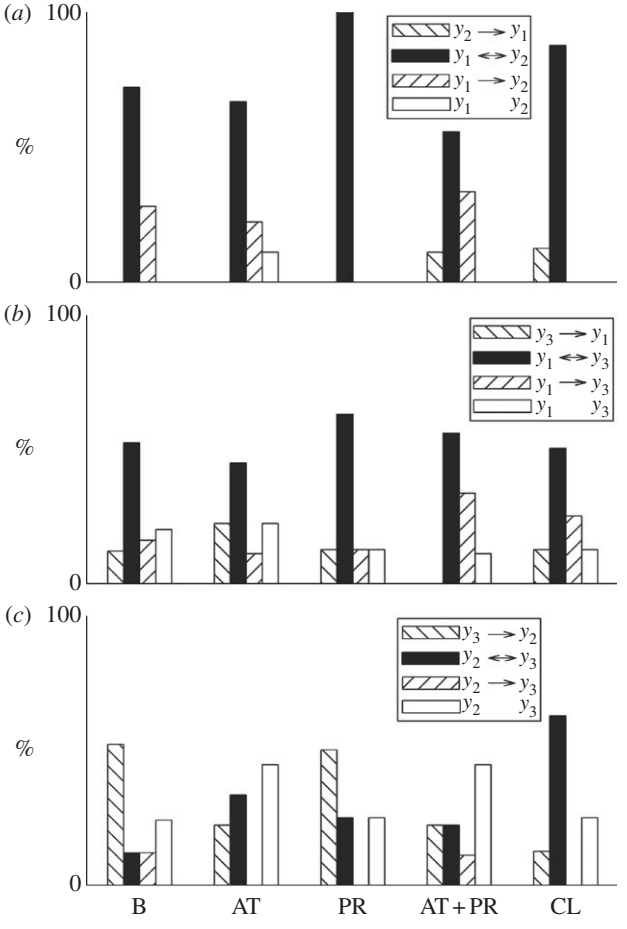

Figure 6. Percentage of (*a*) y_1–y_2, (*b*) y_1–y_3 and (*c*) y_2–y_3 causal interactions at B and after AT, PR, AT + PR and CL with $y_1 =$ hp, $y_2 =$ sap and $y_3 =$ r. The percentage of $y_m \rightarrow y_k$ (backslash-pattern bar), $y_k \leftrightarrow y_m$ (solid bar), $y_k \rightarrow y_m$ (slash-pattern bar) and uncoupled y_k and y_m (open bar) are shown in (*a*) with $m = 2$ and $k = 1$, in (*b*) with $m = 3$ and $k = 1$ and in (*c*) with $m = 3$ and $k = 2$.

and after PR (52% and 50%, respectively). The main effect of AT and AT + PR was to raise the percentage of subjects with uncoupling between y_2 and y_3 compared with B (figure 6*c*, open bar). Conversely, CL increased the probability of finding bidirectional causality between y_2 and y_3 (figure 6*c*, solid bar).

5. Discussion

The main findings of this study can be summarized as follows: (i) at B, HP and SAP interacted in closed loop with a dominant causal direction from HP to SAP; (ii) pharmacological blockades did not alter the bidirectional closed-loop interactions between HP and SAP, but AT reduced the dominance of the causal direction from HP to SAP; (iii) at B, bidirectional interactions between HP and R were frequently found; (iv) the closed-loop relation between HP and R was unmodified by the administration of drugs; (v) at B, unidirectional interactions from R to SAP were often found; and (vi) while AT frequently induced an uncoupling between R and SAP, CL favoured bidirectional interactions.

(a) Effects of pharmacological challenges on heart period–systolic arterial pressure causality

Closed-loop interactions between HP and SAP play a central role in short-term cardiovascular regulation [7,30,32,33]. Indeed, the cardiac mechanics and vascular properties of the arterial tree are both responsible for the causal relation from HP to SAP. Indeed, HP lengthening drives opposite effects on SAP depending on the balance between the positive effects on arterial pressure due to the larger cardiac filling and negative ones driven by a longer diastolic run-off. Cardiac baroreflex feedback is responsible for the reverse causal influence (i.e. from SAP to HP). Deformation of stretch receptors in barosensory vessels induced by SAP changes results in an increased afferent firing to cardiovascular centres in the brainstem and, consequently, to reflex changes of vagal and sympathetic efferent activities directed to the heart, thus driving appropriate HP modifications. This study confirms at B the importance of HP–SAP bidirectional causal interactions in healthy subjects [18,23] and the dominance of the causal relation from HP to SAP over the reverse cardiac baroreflex one [12]. Given the closed-loop relation between HP and SAP, the application of methods assuming an open loop from SAP to HP to estimate baroreflex sensitivity from spontaneous HP and SAP variabilities (i.e. spectral and cross-spectral methods [34,35]) might produce estimates mixing the gain of the feedback and feedforward pathways [16]. The contaminating influences of the feedforward pathway on the estimate of the feedback gain might contribute to the disagreement between the spontaneous and drug-driven baroreflex sensitivity estimates [36].

One of the most important findings of this study is that pharmacological blockades were not able to limit the HP–SAP closed-loop interactions: indeed, the bidirectional causality scheme was the most frequently detected pattern in all the experimental conditions (figure 6*a*). This finding suggests that the autonomic nervous system can solely modulate the dominance of a causal relation with respect to the reverse one (vagal blockade reduces the dominance of causal relation from HP to SAP) but cannot open the HP–SAP closed loop. This conclusion is not entirely new: indeed, during a gradual head-up tilt protocol inducing a progressive vagal withdrawal and sympathetic activation, closed-loop HP–SAP interactions were not affected by the magnitude of the gravitational stimulus, but a progressive shift was observed from a dominant causality from HP to SAP at rest and low tilt table angles to the reverse causality along the cardiac baroreflex pathway (i.e. from SAP to HP) at the highest tilt table inclination [12,18]. Since it is well known that baroreflex sensitivity is under autonomic control, being smaller in the presence of vagal blockade [19] or vagal withdrawal [12] and larger when vagal influences are enhanced [25] or less inhibited by sympathetic blockade [19], these data and those obtained from a gradual head-up tilt protocol [12,18] suggest that causality analysis provides non-redundant information compared

with more traditional analyses involving the assessment of the gain of the HP–SAP relation. In other words, the detection of a significant causal link through causality analysis does not tell us anything about the magnitude of the transformation between input and output (i.e. the gain of the transfer function), but it is a prerequisite for its reliable assessment.

(b) Effects of pharmacological challenges on heart period–respiration causality

The presence of HP variations at the respiratory rate, i.e. the so-called respiratory sinus arrhythmia, suggested a causal link from R to HP. Several mechanisms have been advocated to support the direct causal relation from R to HP. They include the direct coupling between respiratory centres and vagal efferent activities, activation of cardiopulmonary reflexes and direct stimulation of the sinus node tissue [7,37–40]. However, even the reverse causal link was observed (i.e. from HP to R). Several studies reported that central respiratory drive induces changes of HP via variations of the vagal firing preceding modifications of R when measured according to two-belt chest–abdomen inductance plethysmography, thus suggesting a causal link from HP to R [2,7,41,42]. This study supports the hypothesis of bidirectional interactions between HP and R [18]: indeed, at B, a closed-loop relation between HP and R was found in 52 per cent of the subjects and it was the most frequently detected causal pattern (figure 6*b*). The important presence of a causal link from HP to R found in this study is in agreement with the observations made by the earlier studies [2,41,42] even though R was derived using a different technique. This result is not surprising: indeed, the amplitude modulations of the ECG signal, taken as R in this study, are the result of respiratory-related cardiac axis movements synchronous with thoracic movements as monitored in [2,41,42]. The presence of bidirectional interactions between HP and R stresses the need for including the pathway from HP to R in addition to the more frequently modelled link from R to HP [30].

One of the key findings of this study is that the significance of the bidirectional interactions between HP and R remained unmodified after autonomic challenges. A progressive decrease of the direct cardiopulmonary coupling was observed during the gradual vagal withdrawal and sympathetic activation induced by graded head-up tilt test [43], thus suggesting that autonomic control could play a role in modulating the direct causal link from R to HP. In the present study, vagal blockade did not impose an HP–R uncoupling. This result can be interpreted in terms of the dramatic decrease of the HP variance. After AT, the HP variance was reduced to such a level that the direct mechanical effect on the sinus node tissue induced by respiratory-related changes of intrathoracic pressure [37] cannot be dismissed and might represent a significant portion of the respiratory sinus arrhythmia. Therefore, a causal relation from R to HP can be detected. The significance of the causal relation from HP to R is the result of the swiftness of vagal action in driving HP changes compared with the sluggishness of modifications of lung volume inducing respiratory-related movements of cardiac axis, leading to HP changes that precede R variations. Therefore, we expected that vagal blockade could modify the causal link from HP to R. Conversely, the causal relation from HP to R remained significant during AT and AT + PR. This finding suggests that latent variables unaccounted for in the information set (e.g. peripheral resistances) might play a role in determining the relation from HP to R. However, during AT and AT + PR, the bidirectional relations between HP and R might even be the result of the method exploited to derive R series: indeed, given the negligible levels of the HP variance, modifications of QRS morphology due to R might produce measurable effects on HP, thus linking inextricably HP and R series. The negligible effect of β-adrenergic blockade induced by PR and of central sympathetic blockade induced by CL might be related to the inability of the sympathetic system to modulate HP–R causality. Since the limited effect of PR on the gain of the pathway from R to HP is well known [42], this conclusion can be extended to causality. While AT and AT + PR determine a dramatic reduction of the gain of the transfer function from R to HP [7,42], this reduction did not affect either the percentage of subjects with a significant causal link from R to HP or that with bidirectional HP–R interactions. These findings confirmed the independence of causality indices from parameters related to transfer function.

(c) Effects of pharmacological challenges on systolic arterial pressure–respiration causality

At B, an importance presence of the causal relation from R to SAP was found [18] (figure 6*c*). SAP variations at the respiratory rate are the likely result of the respiratory-related fluctuations of intrathoracic pressure modulating right and left preloads and, in turn, stroke volume [44–46]. At B, the negligible causality from SAP to R (or bidirectional SAP–R causality) is expected as well because fast neural actions did not play a role in the relation between R and SAP [7]. Therefore, we can confirm that R is an exogenous source for SAP (i.e. R affects SAP without being affected). This assumption, traditionally exploited in modelling cardiovascular variability interactions [30,32,47], holds better than the same postulate on HP. Since the direct influence of R on SAP (i.e. not mediated by HP changes) is mainly due to the mechanical thoracic coupling between R and vasculature [7,29,32], we expected that the causal relation from R to SAP was not affected by AT and AT + PR. We hypothesize that the uncoupling between SAP and R observed after AT (with or without administration of PR) is the result of the dramatic effects of AT on SAP. The significant increase of SAP due to AT could be able to reduce the driving influences of respiratory-related changes of the intrathoracic pressure on stroke volume and large vessels. PR left unmodified causality from R to SAP since it kept unmodified SAP values compared with B. The administration of CL was able to unveil possible closed-loop circuits between R and SAP. While the action from R to SAP is compatible with a decrease of SAP leading to a more efficient driving effect of respiratory-related changes of intrathoracic pressure on stroke volume and large vessels, the reverse causal link (i.e. from SAP to R) cannot be fully explained given the set of signals used in this study. We suggest that the reduction of the vasomotor tone after CL, influencing blood pressure fluctuations in the low-frequency band without significant variations of HP variability [48], could lead to a spurious detection of causality from SAP to R. However, this hypothesis cannot be tested without including a peripheral vasomotion signal in the information set.

(d) The importance of causality analysis in the assessment of cardiovascular control

Causality analysis provides a unique insight into integrative cardiovascular control under physiological closed-loop conditions. Indeed, it allows the identification of links among variables over predefined temporal directions and the unveiling of the presence of bidirectional interactions (i.e. closed loops). Separation between unidirectional and bidirectional interactions is of paramount importance in the study of cardiovascular control since it allows the distinction between autonomous self-sustained sources driving variability independently of the time course of systemic and peripheral variables (e.g. respiratory centres) and closed-loop mechanisms controlling one variable according to feedforward and feedback pathways (e.g. baroreflex loop). Causality analysis provides non-redundant information with respect to more traditional analyses obtained using monovariate, bivariate or multivariate approaches. Indeed, since it exploits a multivariate approach looking at the joint process, the typical limitation of monovariate approaches (e.g. spectral analysis) linked to the separate description of the dynamics vanishes. As a result of the imposition of a multivariate model, causality analysis is better suited to describe complex interactions than a bivariate approach based on a single-input single-output transfer function. Indeed, the typical assumption of this approach (i.e. the open-loop condition between input and output signals) is relaxed, and a closed-loop relation can be adequately described. In addition, causality analysis provides non-redundant information even with respect to more traditional multivariate model-based analyses focused on the estimation of the transfer function or the impulse responses [47].

Causality analysis can be exploited to limit the complexity of cardiovascular models. Cardiovascular control is formed by a large amount of interacting mechanisms and subsystems [49]. As a consequence, any model trying to give a comprehensive description of cardiovascular control becomes unmanageable and difficult to interpret. Accordingly, traditional models give up the description of the complexity of cardiovascular control and focus their

attention on a few specific mechanisms (e.g. baroreflex regulation). As a drawback of this oversimplified view, complex dynamics are explained in terms of very few mechanisms [50,51]. We propose that a model with minimal complexity could be built by accounting solely for the causal links detected as meaningful by causality analysis. This approach can lead to models of limited complexity but capable of providing insightful parameters due to their non-trivial structure.

(e) Limitations and future developments

The major difficulty in causality analysis lies in creating the information set. If the information set is incomplete, spurious causal links could be detected. Indeed, the model would try to explain interactions according to the signals belonging to the information set. Spurious causal links could be unveiled only if all latent variables were included in the information set. A typical latent variable in several cardiovascular variability studies is R (here included). Only after including R in the information set can the role of baroreflex in governing HP–SAP interactions be reliably described [23]. A trivial solution of the issue of the latent variables is to create an information set including as many signals as possible provided that they do not carry redundant information (i.e. there is no transformation converting a signal, or a combination of signals, into any other belonging to the information set). Unfortunately, this solution is not fully viable because it increases the number of comparisons and the degrees of freedom of the problem, thus decreasing the statistical power of the study. In addition to the completeness of the information set, another major difficulty lies in the variety of signals that, in principle, can equivalently represent the functioning of a specific system. For example, a respiratory signal can be derived from thorax movements using thoracic belts, measurements performed on gas filling a rigid, constant-volume box where the subject is located, respiratory flow measured at the level of the mouth with a flowmeter, intraoesophageal pressure monitored via a small balloon situated in the oesophagus, changes of thoracic impedance assessed through electrodes positioned on the thorax, or ECG amplitude modulations reflecting respiratory-related cardiac axis movements. The choice of the most informative signal for causality analysis requires specific studies recording signals with different techniques and comparing results of causality analysis.

Possible future developments might include: (i) the application of time-varying approaches based on the recursive least-squares algorithms using forgetting factors to deal with the possible presence of non-stationarities and transients [52,53]; (ii) the application of frequency domain techniques to clarify whether specific causal patterns could be associated to particular time scales [54]; and (iii) the application of nonlinear techniques, for example, based on the information domain [55], to understand whether these methods can be helpful in the presence of nonlinearities such as those observed during slow breathing [56] and in pathological conditions [14].

6. Conclusions

This study demonstrates that the analysis of the cardiovascular control based on spontaneous cardiovascular variabilities might benefit from the application of the Granger causality approach in the time domain. Indeed, causality analysis can clarify the type of causal interactions among variables by detecting closed-loop interactions and identifying directionality of the influences. Autonomic blockades suggest the relevance of HP–SAP and HP–R closed-loop interactions and the dependence of the causality pattern between SAP and R on the mean value of SAP. The significance of the approach is accentuated by the non-redundancy of the extracted indices compared with those obtained from more traditional analyses. However, the study suggests that it is worth including the presence of latent variables, such as peripheral resistance, in the information set to complete the universe of knowledge necessary to reliably explain causal relations.

References

1. Angelone A, Coulter NA. 1964 Respiratory sinus arrhythmia: a frequency dependent phenomenon. *J. Appl. Physiol.* **19**, 479–482. (http://jap.physiology.org/content/19/3/479.abstract)
2. Saul JP, Berger RD, Chen MH, Cohen RJ. 1989 Transfer function analysis of autonomic regulation. II. Respiratory sinus arrhythmia. *Am. J. Physiol.: Heart Circ. Physiol.* **256**, H153–H161. (http://ajpheart.physiology.org/content/256/1/H153.abstract)
3. Chess GF, Calaresu FR. 1971 Frequency response model of vagal control of heart rate in the cat. *Am. J. Physiol.* **220**, 554–557. (http://ajplegacy.physiology.org/content/220/2/554.extract)
4. Berger RD, Saul JP, Cohen RJ. 1989 Transfer function analysis of autonomic regulation. I. Canine atrial rate response. *Am. J. Physiol.: Heart Circ. Physiol.* **256**, H142–H152. (http://ajpheart.physiology.org/content/256/1/H142.abstract)
5. Stauss HM, Anderson EA, Haynes WG, Kregel KC. 1998 Frequency response characteristics of sympathetically mediated vasomotor waves in humans. *Am. J. Physiol.: Heart Circ. Physiol.* **274**, H1277–H1283. (http://ajpheart.physiology.org/content/274/4/H1277.abstract)
6. Kawada T, Yanagiya Y, Uemura K, Miyamoto T, Zheng C, Li M, Sugimachi M, Sunagawa K. 2003 Input-size dependence of the baroreflex neural arc transfer characteristics. *Am. J. Physiol.: Heart Circ. Physiol.* **284**, H404–H415. (http://ajpheart.physiology.org/content/284/1/H404.abstract)
7. Saul JP, Berger RD, Albrecht P, Stein SP, Chen MH, Cohen RJ. 1991 Transfer function analysis of the circulation: unique insights into cardiovascular regulation. *Am. J. Physiol.: Heart Circ. Physiol.* **261**, H1231–H1245. (http://ajpheart.physiology.org/content/261/4/H1231.full.pdf)
8. Yamasaki F, Ushida T, Yokoyama T, Ando M, Yamashita K, Sato T. 2006 Artificial baroreflex. Clinical application of a bionic baroreflex system. *Circulation* **113**, 634–639. (doi:10.1161/CirculationAHA.105.587915)
9. Smyth HS, Sleight P, Pickering GW. 1969 Reflex regulation of the arterial pressure during sleep in man. A quantitative method of assessing baroreflex sensitivity. *Circ. Res.* **24**, 109–121. (doi:10.1161/01.RES.24.1.109)
10. Diaz T, Taylor JA. 2006 Probing the arterial baroreflex: is there a 'spontaneous' baroreflex? *Clin. Auton. Res.* **16**, 256–261. (doi:10.1007/s10286-006-0352-5)
11. Granger CWJ. 1969 Investigating causal relations by econometric models and cross-spectral methods. *Econometrica* **37**, 424–438. (doi:10.2307/1912791)
12. Porta A, Catai AM, Takahashi ACM, Magagnin V, Bassani T, Tobaldini E, van de Borne P, Montano N. 2011 Causal relationships between heart period and systolic arterial pressure during graded head-up tilt. *Am. J. Physiol.: Regul. Integr. Compar. Physiol.* **300**, R378–R386. (doi:10.1152/ajpregu.00553.2010)
13. Faes L, Nollo G, Porta A. 2011 Information-based detection of nonlinear Granger causality in multivariate processes via a nonuniform embedding technique. *Phys. Rev. E* **83**, 051112. (doi:10.1103/PhysRevE.83.051112)
14. Nollo G, Faes L, Porta A, Pellegrini B, Ravelli F, Del Greco M, Disertori M, Antolini R. 2002 Evidence of unbalanced regulatory mechanism of heart rate and systolic pressure after acute myocardial infarction. *Am. J. Physiol.: Heart Circ. Physiol.* **283**, H1200–H1207. (http://ajpheart.physiology.org/content/283/3/H1200.abstract)
15. Riedl M, Suhrbier A, Stepan H, Kurths J, Wessel N. 2010 Short-term couplings of the cardiovascualr system in pregnant women suffering from pre-eclampsia. *Phil. Trans. R. Soc. A* **368**, 2237–2250. (doi:10.1098/rsta.2010.0029)
16. Porta A, Furlan R, Rimoldi O, Pagani M, Malliani A, van de Borne P. 2002 Quantifying the strength of the linear causal coupling in closed loop interacting cardiovascular variability signals. *Biol. Cybern.* **86**, 241–251. (doi:10.1007/s00422-001-0292-z)
17. Nollo G, Faes L, Porta A, Antolini R, Ravelli F. 2005 Exploring directionality in spontaneous heart period and systolic arterial pressure variability interactions in humans: implications in the evaluation of baroreflex gain. *Am. J. Physiol.: Heart Circ. Physiol.* **288**, H1777–H1785. (doi:10.1152/ajpheart.00594.2004)
18. Porta A, Takahashi ACM, Catai AM, Montano N. 2013 Assessing causal interactions among cardiovascular variability series through a time domain Granger-causality approach. In *Methods in brain connectivity inference through multivariate times series analysis* (eds L Baccalà, K Sameshima). London, UK: Taylor and Francis.

19. Parlow J, Viale J-P, Annat G, Hughson RL, Quintin L. 1995 Spontaneous cardiac baroreflex in humans: comparison with drug-induced responses. *Hypertension* **25**, 1058–1068. (doi:10.1161/01.HYP.25.5.1058)
20. Soderstrom T, Stoica P. 1988 *System identification*. Englewood Cliffs, NJ: Prentice-Hall.
21. Baselli G, Porta A, Rimoldi O, Pagani M, Cerutti S. 1997 Spectral decomposition in multichannel recordings based on multivariate parametric identification. *IEEE Trans. Biomed. Eng.* **44**, 1092–1101. (doi:10.1109/10.641336)
22. Faes L, Erla S, Porta A, Nollo G. 2013 A framework for assessing frequency domain causality in physiological time series with instantaneous effects. *Phil. Trans. R. Soc. A* **371**, 20110618. (doi:10.1098/rsta.2011.0618)
23. Porta A, Bassani T, Bari V, Pinna GD, Maestri R, Guzzetti S. 2012 Accounting for respiration is necessary to reliably infer Granger causality from cardiovascular variability series. *IEEE Trans. Biomed. Eng.* **59**, 832–841. (doi:10.1109/TBME.2011.2180379)
24. Palus M, Stefanovska A. 2003 Direction of coupling from phases of interacting oscillators: an information-theoretic approach. *Phys. Rev. E* **67**, 055201. (doi:10.1103/PhysRevE.67.055201)
25. Toader E, Cividjian A, Rentero N, McAllen RM, Quintin L. 2008 Cardioinhibitory actions of clonidine assessed by cardiac vagal motoneuron recordings. *J. Hypertens.* **26**, 1169–1180. (doi:10.1097/HJH.0b013e3282fd10e0)
26. Moody G, Mark R, Bump M, Weinstein J, Berman A, Mietus J, Goldberger AL. 1986 Clinical validation of the ECG-derived respiration (EDR) technique. In *Computers in Cardiology 1986, 7–10 October, Boston, MA*, vol. 13, pp. 507–510. IEEE Computer Society Press.
27. Task force of the European Society of Cardiology and the North American Society of Pacing and Electrophysiology. 1996 Standard of measurement, physiological interpretation and clinical use. *Circulation* **93**, 1043–1065. (doi:10.1161/01.CIR.93.5.1043)
28. Eckberg DL. 1976 Temporal response patterns of the human sinus node to brief carotid baroreceptor stimuli. *J. Physiol.* **258**, 769–782. (http://jp.physoc.org/content/258/3/769.long)
29. Cohen MA, Taylor JA. 2002 Short-term cardiovascular oscillations in man: measuring and modelling the physiologies. *J. Physiol.* **542**, 669–683. (doi:10.1113/jphysiol.2002.017483)
30. Baselli G *et al.* 1994 Model for the assessment of heart period and arterial pressure variability interactions and respiratory influences. *Med. Biol. Eng. Comput.* **32**, 143–152. (doi:10.1007/BF02518911)
31. Akaike H. 1974 A new look at the statistical novel identification. *IEEE Trans. Autom. Control* **19**, 716–723. (doi:10.1109/TAC.1974.1100705)
32. De Boer RW, Karemaker JM, Strackee J. 1987 Hemodynamic fluctuations and baroreflex sensitivity in humans: a beat-to-beat model. *Am. J. Physiol.: Heart Circ. Physiol.* **253**, H680–H689. (http://ajpheart.physiology.org/content/253/3/H680.abstract)
33. di Rienzo M, Castiglioni P, Mancia G, Pedotti A, Parati G. 2001 Advancements in estimating baroreflex function. *IEEE Eng. Med. Biol. Mag.* **2**, 25–32. (doi:10.1109/51.917721)
34. Pagani M, Somers VK, Furlan R, Dell'Orto S, Conway J, Baselli G, Cerutti S, Sleight P, Malliani A. 1988 Changes in autonomic regulation induced by physical training in mild hypertension. *Hypertension* **12**, 600–610. (doi:10.1161/01.HYP.12.6.600)
35. Robbe HWJ, Mulder LJM, Ruddel H, Langewitz WA, Veldman JBP, Mulder G. 1987 Assessment of baroreceptor reflex sensitivity by means of spectral analysis. *Hypertension* **10**, 538–543. (doi:10.1161/01.HYP.10.5.538)
36. Lipman RD, Salisbury JK, Taylor JA. 2003 Spontaneous indexes are inconsistent with arterial baroreflex gain. *Hypertension* **42**, 481–487. (doi:10.1161/01.HYP.0000091370.83602.E6)
37. Bernardi L, Keller F, Sanders M, Reddy PS, Griffith B, Meno F, Pinsky R. 1989 Respiratory sinus arrhythmia in the denervated human heart. *J. Appl. Physiol.* **67**, 1447–1455. (http://jap.physiology.org/content/67/4/1447.abstract)
38. Eckberg DL. 2003 The human respiratory gate. *J. Physiol.* **548**, 339–352. (doi:10.1113/jphysiol.2002.037192)
39. Gilbey MP, Jordan D, Richter DW, Spyer KM. 1984 Synaptic mechanisms involved in the inspiratory modulation of vagal cardio-inhibitory neurones in the cat. *J. Physiol.* **356**, 65–78. (http://jp.physoc.org/content/356/1/65.long)
40. Hakumaki MOK. 1987 Seventy years of the Bainbridge reflex. *Acta Physiol. Scand.* **130**, 177–185. (doi:10.1111/j.1748-1716.1987.tb08126.x)
41. Perrott MH, Cohen RJ. 1996 An efficient approach to ARMA modeling of biological systems with multiple inputs and delays. *IEEE Trans. Biomed. Eng.* **43**, 1–14. (doi:10.1109/10.477696)

42. Yana K, Saul JP, Berger RD, Perrott MH, Cohen RJ. 1993 A time domain approach for the fluctuation analysis of heart rate related to instantaneous lung volume. *IEEE Trans. Biomed. Eng.* **40**, 74–81. (doi:10.1109/10.204773)
43. Porta A, Bassani T, Bari V, Tobaldini E, Takahashi ACM, Catai AM, Montano N. 2011 Model-based assessment of baroreflex and cardiopulmonary couplings during graded head-up tilt. *Comput. Biol. Med.* **42**, 298–305. (doi:10.1016/j.compbiomed.2011.04.019)
44. Caiani E, Turiel M, Muzzupappa S, Porta A, Baselli G, Pagani M, Cerutti S, Malliani A. 2000 Evaluation of respiratory influences on left ventricular function parameters extracted from echocardiographic acoustic quantification. *Physiol. Meas.* **21**, 175–186. (doi:10.1088/0967-3334/21/1/321)
45. Innes JA, De Cort SC, Kox W, Guz A. 1993 Within-breath modulation of left ventricular function during normal breathing and positive-pressure ventilation in man. *J. Physiol.* **460**, 487–502. (http://jp.physoc.org/content/460/1/487.long)
46. Toska K, Eriksen M. 1993 Respiration-synchronous fluctuations in stroke volume, heart rate and arterial pressure in humans. *J. Physiol.* **472**, 501–512. (http://jp.physoc.org/content/472/1/501.long)
47. Mullen TJ, Appel ML, Mukkamala R, Mathias JM, Cohen RJ. 1997 System identification of closed-loop cardiovascular control: effects of posture and autonomic blockade. *Am. J. Physiol.: Heart Circ. Physiol.* **272**, H448–H461. (http://ajpheart.physiology.org/content/(272/1/H448.abstract)
48. Castiglioni P, Parati G, di Rienzo M, Carabalona R, Cividjian A, Quintin L. 2011 Scale exponents of blood pressure and heart rate during autonomic blockade as assessed by detrended fluctuation analysis. *J. Physiol.* **589**, 355–369. (doi:10.1113/jphysiol.2010.196428)
49. Koepchen HP. 1991 Physiology of rhythms and control systems: an integrative approach. In *Rhythms in physiological systems* (eds H Haken, HP Koepchen), pp. 3–20. Berlin, Germany: Springer.
50. Burgess DE, Hundley JD, Li S-G, Randall DC, Brown DR. 1997 First-order differential-delay equation for the baroreflex predicts the 0.4 Hz blood pressure rhythm in rats. *Am. J. Physiol.: Regul. Integr. Compar. Physiol.* **273**, R1878–R1884. (http://ajpregu.physiology.org/content/273/6/R1878.abstract)
51. Mrowka R, Persson PB, Theres H, Patzak A. 2000 Blunted arterial baroreflex causes 'pathological' heart rate turbulence. *Am. J. Physiol.: Regul. Integr. Compar. Physiol.* **279**, R1171–R1175. (http://ajpregu.physiology.org/content/279/4/R1171.abstract)
52. Hesse W, Moller E, Arnold M, Schack B. 2003 The use of time-variant EEG Granger causality for inspecting directed interdependencies of neural assemblies. *J. Neurosci. Methods* **124**, 27–44. (doi:10.1016/S0165-0270(02)00366-7)
53. Sommerlade L, Thiel M, Platt B, Piano A, Riedel G, Grebogi C, Timmer J, Schelter B. 2012 Inference of Granger causal time-dependent influences in noisy multivariate time series. *J. Neurosci. Methods* **203**, 173–185. (doi:10.1016/j.jneumeth.2011.08.042)
54. Chicharro D. 2011 On the spectral formulation of Granger causality. *Biol. Cybern.* **105**, 331–347. (doi:10.1007/s00422-011-0469-z)
55. Hlavackova-Schindler K, Palus M, Vejmelka M, Bhattacharya J. 2007 Causality detection based on information-theoretic approaches in time series analysis. *Phys. Rep.* **441**, 1–46. (doi:10.1016/j.physrep.2006.12.004)
56. Porta A, Baselli G, Guzzetti S, Pagani M, Malliani A, Cerutti S. 2000 Prediction of short cardiovascular variability signals based on conditional distribution. *IEEE Trans. Biomed. Eng.* **47**, 1555–1564. (doi:10.1109/10.887936)